Woodchip-filled trenches: A solution to enhance urban water infiltration capacity?

P. Louis, L. Delgado-Gonzalez, L. Lassabatère, S. Czarnes, J. Aubert, A. Imig, R. Clément

Geoderma 451 (2024) 117057

Contents lists available at ScienceDirect

Geoderma

journal homepage: www.elsevier.com/locate/geoderma

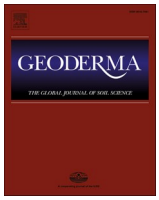

Woodchip-filled trenches: A solution to enhance urban water infiltration capacity?

P. Louis [a], L. Delgado-Gonzalez [a], L. Lassabatère [b], S. Czarnes [c], J. Aubert [a], A. Imig [a], R. Clément [a,*]

[a] INRAE UR REVERSAAL, 5 Rue de la Doua, CS 20244 69625, Villeurbanne Cedex, France
[b] Univ Lyon, Université Claude Bernard Lyon 1, CNRS, ENTPE, UMR 5023 LEHNA, Vaulx-en-Velin, 69518, France
[c] Université Claude Bernard Lyon 1, Laboratoire d'Écologie Microbienne, UMR CNRS 5557, UMR INRAE 1418, VetAgro Sup, 69622, Villeurbanne, France

ARTICLE INFO

Handling Editor: Jingyi Huang

Keywords:
Greywaters
Infiltration tests
Saturated hydraulic conductivity
Drainage material
Beerkan tests
Earthworm abundance
BEST methods

ABSTRACT

Urban water management has been increasingly relying on infiltration to limit the environmental impact of stormwater, secondary treated effluent and gray water. The infiltration systems used are generally based on non-renewable drainage materials featuring a pronounced ecological footprint (i.e., excavation and transport), such as gravel. This paper investigates the possibility of using woodchips instead of traditional drainage materials. Our study examines flow dynamics in woodchip-filled infiltration trenches at four decentralized gray water sites, on a silty clay soil. Infiltration tests were conducted using the Beerkan method to measure soil infiltration capacity both beneath the woodchip-filled trenches and in adjacent soil. Soil hydraulic functions were determined according to the BEST method, then comparisons were drawn between the woodchip-filled trench and natural soil. Results indicate that woodchips locally maintain or enhance soil infiltration rates, with a hydraulic conductivity up to 200 times higher in woodchip-treated soil. Additional soil measurements and analyses serve to formulate hypotheses on how the woodchips actually contribute to these effects. Dye tracer experiments revealed preferential pathways facilitated by macro fauna (earthworms) and, most likely, plant roots. This last information input has been corroborated since earthworm counts did prove to be significantly higher in the woodchips than in the soil. A chemical analysis of the soils also showed a significant enrichment of carbon and nitrogen under the trench, which may also improve soil structure and stability and perhaps indirectly enhance water infiltration capacity. In summary, the presence of woodchips in infiltration trenches improves the soil hydraulic conductivity at saturation for systems that have been in use for 5 to 10 years. These findings underscore the potential of woodchips in sustainable urban water management in order to enhance the functionality and efficiency of drainage materials by means of limiting the clogging effect.

1. Introduction

In order to improve Urban Water (UW) management, the reliance on water infiltration is becoming increasingly common, whether for stormwater (SW) management (Sharma and Malaviya, 2021), secondary treated effluent (STE) from wastewater treatment plants (Delgado-Gonzalez et al., 2023) or gray water from decentralized systems (Boano et al., 2020). The UW infiltration process involves the discharge of water over a surface like trenches, ponds, basins or meadows, allowing for gradual infiltration through the soil (Rabouli et al., 2021). This process is conducted to both improve water quality and preserve the receiving environments, thus ensuring a sustainable use of water resources. UW infiltration provides many benefits (D'Aniello et al., 2019), namely: i) reducing flooding and improving ecological resilience and water quality; ii) regulating the urban climate, by the irrigation of green surfaces (reducing heat islands); iii) reinforcing the stability of buildings, by preventing soil settlement through maintained soil moisture levels; and iv) contributing to groundwater recharge.

However, the infiltration of large UW volumes leads over time to clogged soils (Assouline and Narkis, 2011). Soil clogging can occur whenever UW contains high levels of suspended solids. These solids accumulate in the soil, clogging the soil pores, or accumulating at the soil surface, and reducing the rate of infiltration, which in turn may lead to water ponding at the soil surface and even to system failure. In the

* Corresponding author.
E-mail address: remi.clement@inrae.fr (R. Clément).

https://doi.org/10.1016/j.geoderma.2024.117057
Received 29 March 2024; Received in revised form 2 September 2024; Accepted 4 October 2024
Available online 12 October 2024

case of STE or gray water infiltration, clogging can also be biological due to the presence of microorganisms (Bisone et al., 2017). Wastewater infiltration is typically facilitated by drainage materials. Non-renewable drainage materials, such as sand, pebbles or gravel, are used to ensure effective water distribution within the infiltration zone (Chahar et al., 2012; Rabouli et al., 2021). Nevertheless, these materials do not prevent clogging over time, in particular at the interface between the drainage materials and the soils below.

Stakeholders are now considering the replacement of non-renewable drainage materials with biodegradable and renewable options, such as woodchips, for the infiltration surfaces of gray water (Brun et al., 2021). Woodchips are small- to medium-sized pieces of wood produced by cutting or chipping larger wood pieces from trees, branches, logging residues, and other wood waste (Maboeta and Rensburg, 2003). This material offers two main advantages: 1) high capillarity, providing excellent water retention capacity; and 2) beneficial impacts on the soil structure beneath the woodchips (Fontana et al., 2023), potentially enhancing water infiltration. In this study, we hypothesize that using woodchips in woodchip-filled trenches (WcT) positively impacts the soil and its infiltration capacity for several reasons. Firstly, the degradation of woodchips is expected to contribute organic matter to the soil. Organic matter promotes an open soil structure and increases its hydraulic conductivity (Nemes et al., 2005; Rawls et al., 2004). Secondly, the input of organic matter and nutrients is anticipated to promote biodiversity, particularly through bioturbating species like earthworms and *collembola* (Maboeta and Rensburg, 2003). Woodchips provide a suitable habitat for soil organisms and macrofauna, fostering their development, which may enhance bioturbation (Blouin et al., 2013). Lastly, the degradation of woodchips is expected to provide nutrients, favoring the growth of plants and their root systems. The combination of these three factors is expected to positively impact the soil beneath the woodchips, increasing its hydraulic conductivity and infiltration capacity. This, in turn, should limit the risks of soil clogging by UW infiltration and related system dysfunction. Consequently, using woodchips on infiltration surfaces could help maintain UW infiltration capacity, although no references currently exist in the literature on this issue.

The aim of this paper therefore is to demonstrate that the use of woodchips improves and maintains the capacity of soils to infiltrate water below the infiltration surface and enhances the functionality and efficiency of drainage materials. In addition, this paper identifies the mechanisms involved in maintaining infiltration. Our work has been based on a case study, with WcT being used for gray water infiltration in four decentralized systems, set up as experimental sites. The four systems include two older systems, functioning for 9–11 years, which allow for the assessment of long-term impacts of woodchips, and two newer systems, functioning for 5–6 years, which provide insights into the short-term impacts.

2. Materials and methods

2.1. General methodology

The methodology proposed herein to assess the impact of woodchips on soil infiltration behavior and capacity is primarily based on field experiments. It comprises four steps:

1) Quantification of the infiltration capacity of soils underneath the infiltration WcT and in the natural native soils (also referred to as “reference soils”) at the same depth by means of infiltration tests (Beerkan method). The cumulative infiltrations are then modeled with the Beerkan Estimation of Soil Transfer (BEST) parameters method (Angulo-Jaramillo et al., 2019) in order to calculate the saturated hydraulic conductivity (Ks).
2) Brilliant Blue dye tracer experiments in complement to infiltration experiments. At the end of the infiltration period, soil pits are employed to observe both the flow paths and the soil structure beneath the WcT.
3) Soil sampling to compare physicochemical properties between the soils under the WcT and the natural soils.
4) Enumeration of the macrofauna, in particular of earthworms in the natural soils and below the WcT.

2.2. Study sites

The experimental campaign was carried out in southwestern France (county of Gers) in 2021. Four study sites were selected (see Fig. 1a). All sites contain infiltration trenches filled with woodchips for decentralized gray water treatment plants designed for onsite sanitation. The sizing of woodchip-filled trenches is typically determined by allocating 1 m^2 of surface area per inhabitant.

The trenches are typically fed by a single infiltration point at the origin of the trench, with the drainage material (in this case woodchips) ensuring the dispersion of the water (Fig. 1b). The system is designed with several trenches, to ensure alternating feeding, thus allowing the soil to recover between successive infiltrations and limiting the risk of clogging. For the examples in Fig. 1c, Trench 1 (shown in green) is fed during the first period, while the three other trenches (in blue) are at rest. These sites were chosen based on various criteria, including soil and woodchip type, gray water quality and commissioning date (Table 1). The main criteria that guided our choice include: soils with low permeability that may be prone to clogging, the use of ramial chipped wood (RCW) for the woodchips, and experimental sites with a minimum 3-year activity period.

These four sites exhibit different soil characteristics. Sites 3 and 4 lie close to one another and are located in the same village. The main characteristics of the surface soil (top 0–20 cm) were measured by the Soil Analysis Laboratory (LAS, INRAE, Arras, France) (Table 2).

These types of soil are generally recognized to have a low hydraulic conductivity at saturation, on the order of 10^{-5} to 10^{-8} $m.s^{-1}$ (Carsel and Parrish, 1988). Moreover, our study selected sites that had been in operation for 5 to 13 years so as to observe the long-term impact of woodchips on soils. The daily hydraulic load is low, on the order of 16 to 46 $mm.d^{-1}$. The trenches were filled with ramial woodchips (i.e., non-resinous materials).

2.3. Hydraulic parameters and infiltration capacity

2.3.1. Infiltration tests and experimental set-up

The first step involves characterizing the hydraulic conductivity at saturation of the reference (natural native) soil as well as the soil under the WcT at each site. The infiltration tests were performed in both the WcT and reference soil. When carrying out the infiltration tests in the WcT, all woodchips were removed (about 0.3 m or 0.4 m deep depending on the study site) to enable testing the soil. In the reference soil, the first 0.3 m or 0.4 m of depth were also carefully removed, to enable testing the same soil horizon. These tests were performed in two WcT for each study site and at two locations in the WcT. For the reference soil, measurements were recorded at a lateral distance of 1.20 m from the WcT, and at a distance from the feeding of 0.6 m and 1.6 m (Fig. 2). These tests are based on the Beerkan method (Braud et al., 2005), which is a simple and low-cost method to measure the cumulative infiltration at surface and (Nemes et al., 2005; Rawls et al., 2004) estimates the soil hydraulic properties (water retention and hydraulic conductivity functions) when combined with the BEST algorithm. This method entails use of a small cylindrical ring (usually made of steel) 150 mm in diameter and 80 mm high inserted into the soil at a specific depth (~0.5 cm). The ring is then filled with several known volumes of water, and the time required for the infiltration of each volume is noted. Next, the cumulative infiltration is defined by assigning to each infiltration time the height of infiltrated water, i.e., the infiltrated volume divided by the area of the infiltration surface. The Beerkan method has been

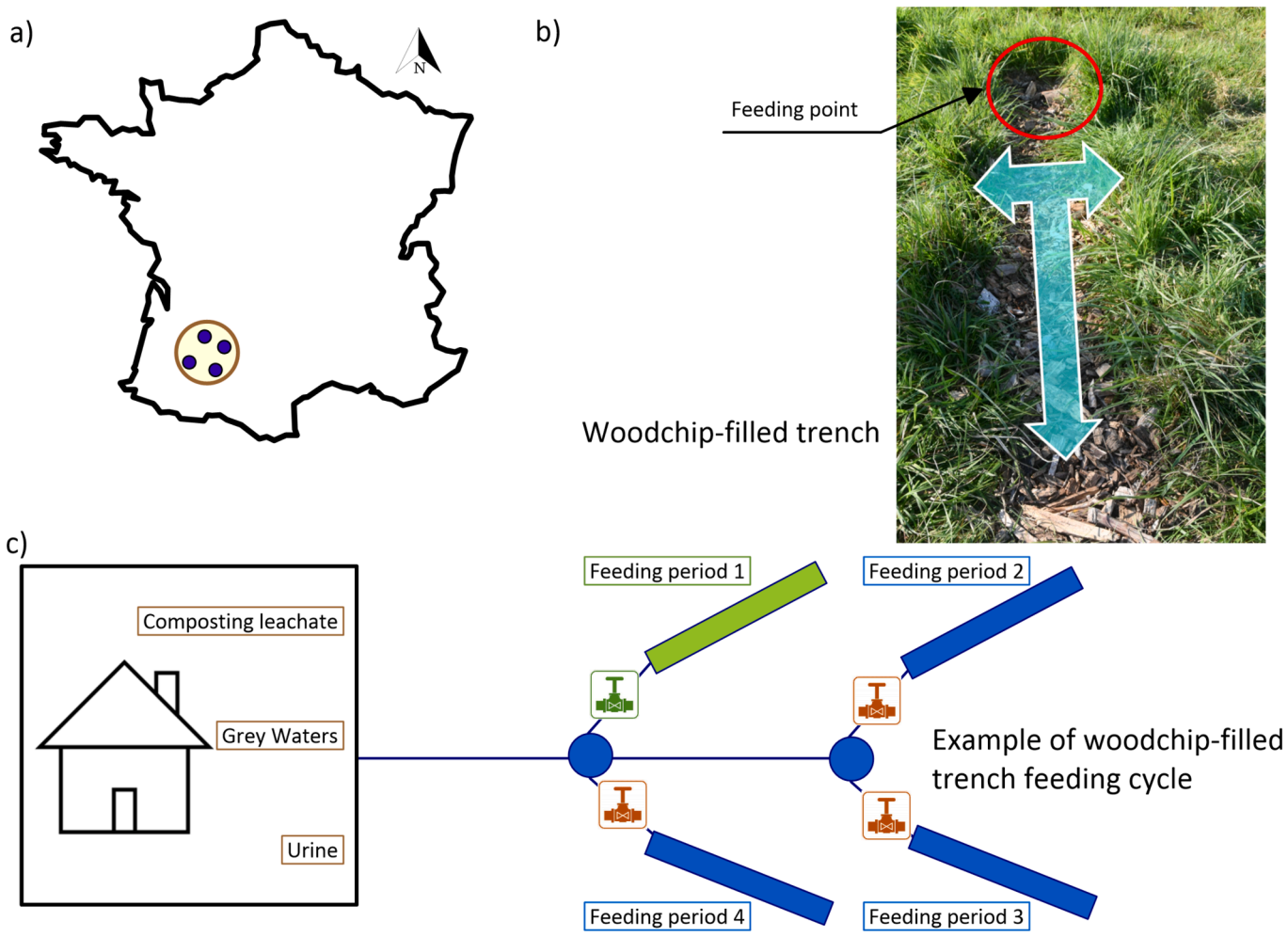

Fig. 1. Description of study sites: a) localization of the study site, b) photograph of woodchip-filled trenches, c) schematic of a woodchip-filled trench infiltration system used in decentralized sanitation.

Table 1
Woodchip-filled trench characteristics at the study sites.

	Site 1	Site 2	Site 3	Site 4
Commissioning date	2018	2015	2019	2013
Design parameter [m^2.PE^{-1}]	1	1.88	1	1.45
Infiltration area (m^2)	3	7.5	4	2.07
Number of trenches [-]	3	5	4	3
Dimensions (w x L x d, [m])	0.4 x 2.5 x 0.3	0.3 x 5 x 0.2	0.4 x 2.5 x 0.3	0.3 x 2.3 x 0.4
(Waste)water type	Gray Water + Urine			
Estimated hydraulic load [$mm.d^{-1}$]	46	16	17	49
Alternation: feeding period (week)	1	2	6	14
Alternation: resting period (week)	2	8	6	28
Woodchip type	RCW			
Year of last woodchip refill	2018	2020	2019	2019

adapted to an automatic infiltrometer system, called the Beerkan Automatic Method (BAM). BAM was pioneered by Di Prima et al. (2016) and more recently improved by Concialdi et al. (2020). An automated device replaces the operator and supplies water automatically. More information on the infiltrometer device and protocol of use may be found in Concialdi et al. (2020).. The various measurements yield the cumulative infiltration as a function of time for each infiltration test.

Table 2
Soil characteristics at the study sites.

		Site 1	Site 2	Site 3	Site 4
Type	**Standard**	Luvisol	Calcosol	Neoluvisol	Neoluvisol
Sand (%)	**NF X31-107**	29	6	25	15
Silt (%)	**(2003)**	59	38	59	57
Clay (%)		12	56	23	28
CaCO3 (g. kg^{-1})	**ISO 10,693 (1995)**	<1	41	<1	<1
pH (H2O)	**ISO 10,390 (2021)**	7	9.7	5.9	5.9
CEC (cmol+/ kg)	**NF X31-130 (199)**	3.61	8.5	6.89	7.47
Organic carbon (g. kg^{-1})	**ISO 10,694 (1995)**	2.8	1.7	12.4	13.6

2.3.2. *BEST data analysis*

As proposed by Lassabatere et al. (2019), each cumulative infiltration has been treated using the three BEST methods (Slope, Intercept and Steady-state), as developed respectively by Lassabatere et al. (2006), Yilmaz et al. (2010), and Bagarello et al. (2014). These methods consider that the water retention function is described by the van Genuchten model (van Genuchten, 1980) along with Burdine's condition (m = 1—2/n), and hydraulic conductivity is described by the Brooks and Corey relationship (Brooks and Corey, 1964), with the exponent $\eta = 2/(m\ n) + 3$. All three methods assume that the residual water

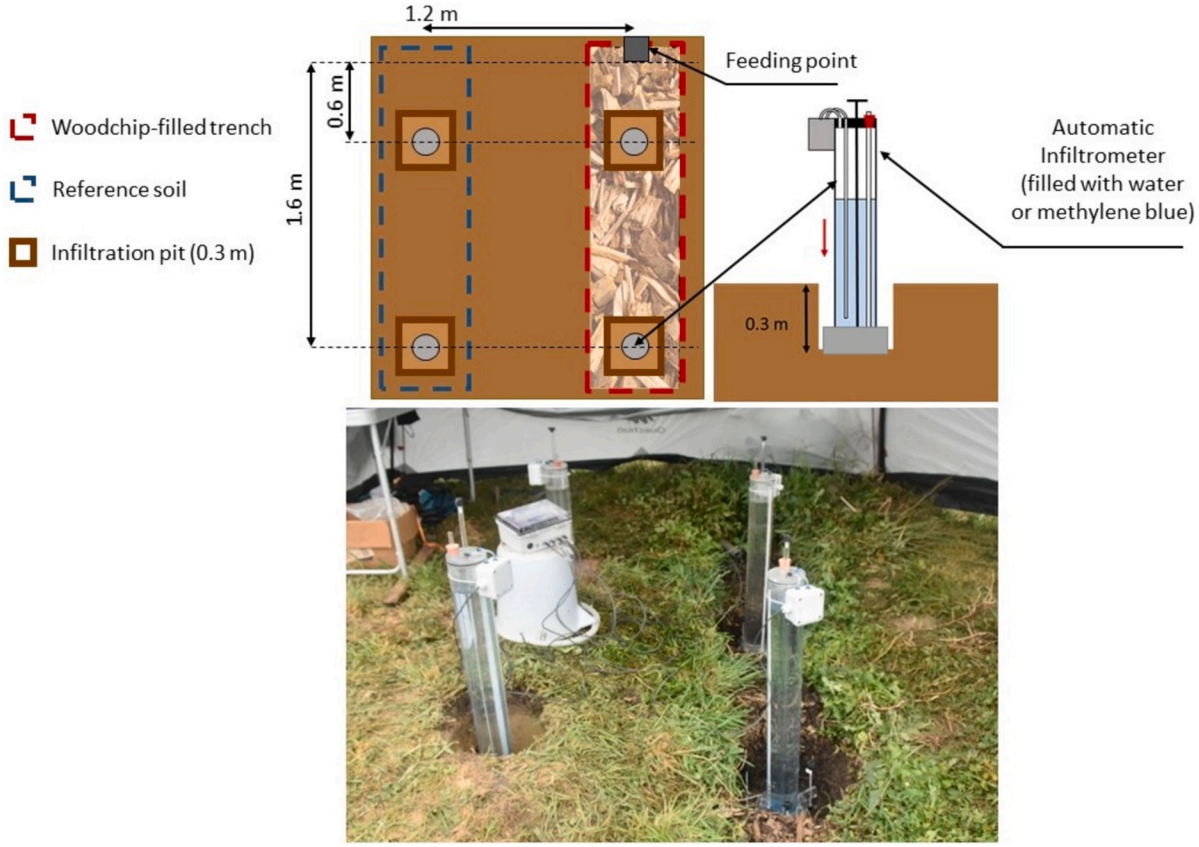

Fig. 2. Infiltration tests based on the Beerkan method in both the reference soil and Woodchip-filled trenches.

content equals zero and moreover that the saturated water content equals soil porosity. The three methods treat the particle size distribution by use of the pedotransfer functions (PTFs) developed in Lassabatere et al. (2006) in order to derive the shape parameters n, m and η. The three models utilize infiltration data to derive both the soil sorptivity, S [L $T^{-0.5}$], and saturated soil hydraulic conductivity, Ks [L T^{-1}], before determining the scale parameter for the water pressure head, hg [L]. The difference between the three methods stems from their approaches to fitting the experimental cumulative infiltration to the approximate expansions for transient and steady states, as defined by Haverkamp et al. (1994), as well as their approaches to deriving S, Ks and hg. More specifically, BEST-Slope uses the slope of the straight line defined by the last points (representative of the steady state) to link S with Ks, before fitting the transient model to the experimental data solely by optimizing S. BEST-Intercept uses the intercept of the straight line defined by the last points to relate S and Ks, before fitting the transient model to the experimental data solely by optimizing S. Lastly, BEST-Steady-state relies on both the intercept and slope of the straight line defined by the last points to resolve a set of two equations, leading to the estimation of the two unknowns. Once S and Ks have been determined, hg can be derived, as described in Lassabatere et al. (2006). The different structures of the three BEST methods make them sensitive to different kinds of input errors (Lassabatere et al., 2019). The three methods provide similar estimates when used with error-free numerically generated data. However, with real experimental data, the methods may yield different estimates for the scale parameters. Consequently, Angulo-Jaramillo et al. (2019) suggested running all three methods and averaging their estimates, which was done in this study. Further details on their design and application can be found in Angulo-Jaramillo et al. (2019).

We verified that the estimates for both hg, the scale parameter for water pressure head, and Ks were normally distributed, in using the QQ plot and Kolmogorov-Smirnov test as suggested by Lassabatere et al. (2019). Next, for each run, the parameter values were estimated by considering the arithmetic average of the three different estimates obtained with the BEST-Slope, BEST-Intercept and BEST-Steady-state methods. Depending on the reliability of the field data acquired at our study sites and the conditions necessary to introduce them when running the three different BEST methods, a number of outliers were discarded. The infiltration parameter values presented in this paper are therefore the mean values obtained on the non-outlier values. To evaluate the difference of Ks between WcT and soil, we calculated an increase rate (IR):

$$IR = (Ks_{WcT} - Ks_{avsoil})*100/Ks_{avsoil}$$

Where Ks_{WcT} is the Ks of the WcT and Ks_{avsoil} is the average soil Ks on studied site.

2.4. Dye tracer and imaging for extracting infiltration pattern

To characterize the spatial patterns of flow pathways, dye tracer experiments were conducted on a qualitative basis along with a few infiltration tests, in order to trace water flows into the soils below the woodchip-filled trenches. As proposed by Flury and Flühler (1994), Brilliant Blue FCF was used as the tracer because it is highly visible, nontoxic to the environment and behaves as a good tracer of water with very low retardation factors (i.e., no sorption). Infiltration tests with Brilliant Blue were carried out in the soil beneath the wood chips after the wood chips had been removed from the trench. The infiltrometer was approximately filled with 5 l of water, in which 10 g of Brilliant Blue FCF were dissolved. Upon completion of the infiltration tests, soil pits were dug 0.4 m deep to observe the pattern of flow pathways below the infiltrometers. For each pit, soil slices were then captured using a camera (Samsung SM-G930F, 12.2 MP, 35 mm f/1.7). Next, we analyzed the pictures using the open-source Python PIL library (htt

ps://github.com/python-pillow/Pillow/tree/9.5.0) and Open CV (https://opencv.org/), for the purpose of extracting a binary image of the tracer from the pictures. Given the different workflows for this type of analysis (Schneider et al., 2018), we chose the following strategy:

- Distortion and radial correction
- Correction for white balance
- Improvement of image sharpness
- Application of a segmentation strategy, based on K-means with 5 clusters
- Extraction of the cluster representing the plot in a binary image.

2.5. Soil sampling and analytical methods

To determine the effect of woodchips on the physical and chemical properties of soils, we monitored the following parameters: bulk density and soil porosity, water content, Total Organic Carbon (TOC), Total Nitrogen (TN), total phosphate (TP), pH, and salinity. For sampling purposes, the bottom of the trench is considered to be level 0. For each of the study sites, reference soil was sampled below the level 0 at various depths (0–5 cm, 5–10 cm and 10–20 cm). Soil samples were also extracted underneath the woodchips, at the same depths as for the reference soil, and at two other locations, i.e., 60 cm and 160 cm from the feeding point, for a total of 9 samples per site. For the physical analyses such as porosity, water content and density, the undisturbed cores were sampled with cylinders under the infiltrometers after the infiltration tests. Subsequently, the cylinders were hermetically sealed and taken to the laboratory for further analyses. These cylinders had a diameter of 5.5 cm and a height of 4 cm. For the physicochemical parameters (TOC, TN, TP, pH, salinity), we extracted about 500 g of disturbed soil under the infiltrometer.

2.5.1. Total porosity, volumetric water content and density

Cored soil samples were weighed on laboratory scales with a resolution of 1 mg. The samples were then slowly saturated for two days. The cylindrical soil samples were weighed to obtain the weight at saturation. Next, after draining, the samples were placed into a laboratory dryer and dried for 24 h at 105 °C. After drying, the samples were weighed once again. The volumetric content and porosity could be calculated from the difference between the two weights by taking into account the mineral particle and water densities (Hillel, 1980).

2.5.2. TOC, TN, TP

A number of indicators were used to measure soil quality, including bulk density or porosity, organic matter content, TN), TP and calcium (Ca), as well as cation exchange capacity (CEC), C/N ratio and pH (Taylor et al., 2010; Bünemann et al., 2018). Prior to analysis, the soil samples were air dried, disaggregated, sieved to 2 mm and then ground in order to obtain a granulometry < 250 μm. Total carbon and total nitrogen contents were determined by means of dry combustion methods (receptively ISO 14235 and ISO 13878). When the samples contained significant amounts of carbonates ($CaCO_3 > 1$ g/kg), a sample correction step was performed. To measure total phosphorus (TP) content, the samples were previously charred at 450 °C and mineralized in a mixture of hydrofluoric and perchloric acids (NF X 31–147 (1996), and ISO 14869–1). The phosphorus measurement was conducted by use of inductively coupled plasma atomic emission (ICP-AES, NF ISO 22036).

2.5.3. Abundance of earthworms

Earthworms were counted to compare abundance between the reference soil and the soil under the WcT. The earthworms were extracted from the woodchips and soil via a mechanical method, in a 0.3 m x 0.3 m square surface (after removal of the surface vegetation for the reference soil). A manual extraction was performed by digging to a depth of 0.3 m; the worms from these manual extractions were then isolated and counted. No species identification was carried out, but merely a count per volume of soil.

3. Results

3.1. Infiltration tests and saturated hydraulic conductivity from the BEST methods

Fig. 3 shows the cumulative infiltration curves obtained in the reference soil and below the WcT at the 4 study sites. All sites do not feature the same number of curves, depending on the outliers discarded thedata analysis (2 outliers for Site 2, 1 for Site 3 and 1 for Site 4).

1. Site 1: under the WcT, a cumulative infiltration of 100 mm is reached between 110 and 1200 s depending on the trench, with an apparent infiltration rate between 265 and 2,655 mm h^{-1} at the end of the experiment; whereas 100 mm of cumulative infiltration is never attained for the reference soils after 7700 s, with an apparent infiltration rate of 3 mm h^{-1}.
2. Site 2: under the WcT, a cumulative infiltration of 100 mm is reached between 1900 and 3700 s, with an apparent infiltration rate between 98 and 172 mm h^{-1} at the end of the experiment; whereas 100 mm of cumulative infiltration is never attained for the reference soils after 6500 s, with an apparent infiltration rate of 24 mm h^{-1}.
3. Site 3: under the WcT, a cumulative infiltration of 100 mm is attained between 280 and 500 s, for an apparent infiltration rate of between 648 and 1171 mm h^{-1}. Two infiltration tests (out of 3) in the reference soil exceed 100 mm of cumulative infiltration, in 4800 and 5800 s respectively, with an apparent infiltration rate between 8 and 118 mm h^{-1} at the end of the experiment.
4. Site 4: under the WcT, a 100-mm cumulative infiltration is attained between 200 and 800 s, with an apparent infiltration rate of between 316 and 1419 mm h^{-1}. The two infiltration tests in the reference soil exceed 100 mm of cumulative infiltration, in 790 and 830 s respectively, with apparent infiltration rates of 359 and 430 mm h^{-1} at the end of the experiment.

The differences observed between WcT and soil are significant overall, as the sensor used is accurate to less than 1 mm. For Sites 1, 2 and 3, the infiltration capacity of the soils increases when woodchips are used. For Site 4, the soil infiltration capacity is at least maintained, with values slightly higher on average for the WcT. Although no replicates were produced at the sites, each study site shows infiltration curves with no clear difference between infiltration into the WcT near the feed point ($d = 0.6$ m) or far from it ($d = 1.6$ m), except the case of Site 4, with larger differences between the two distances.

All infiltration curves display a concave part followed by a linear part, corresponding respectively to the transient and steady states of infiltration. Consequently, we expected the BEST methods to be feasible for calculating the infiltration parameters. That was the case and most of the cumulative infiltrations could be treated with the BEST methods. We reported the estimations for the saturated hydraulic conductivity in Table 3. The hydraulic conductivity at saturation is much higher under the WcT, particularly for Sites 1 and 2. This variation is less pronounced for Site 3, and the values are even equivalent to those of the reference soil for Site 4, indicating no significant effect of the WcT. These observations are reflected by the increase in hydraulic conductivity as a percentage of the average value for the reference soil (IR). Apart from Site 4, the saturated hydraulic conductivity increased by at least 82 %, with increases reaching as high as 19216 %. Only Site 4 had lower saturated hydraulic conductivity under the WcT.

3.2. Dye tracer and soil pit

The second step consisted of carrying out 4-dye tracer experiments in the woodchip-filled trenches in conjunction with the infiltration tests. Fig. 4 presents the results of the propagation of the Brilliant Blue tracer;

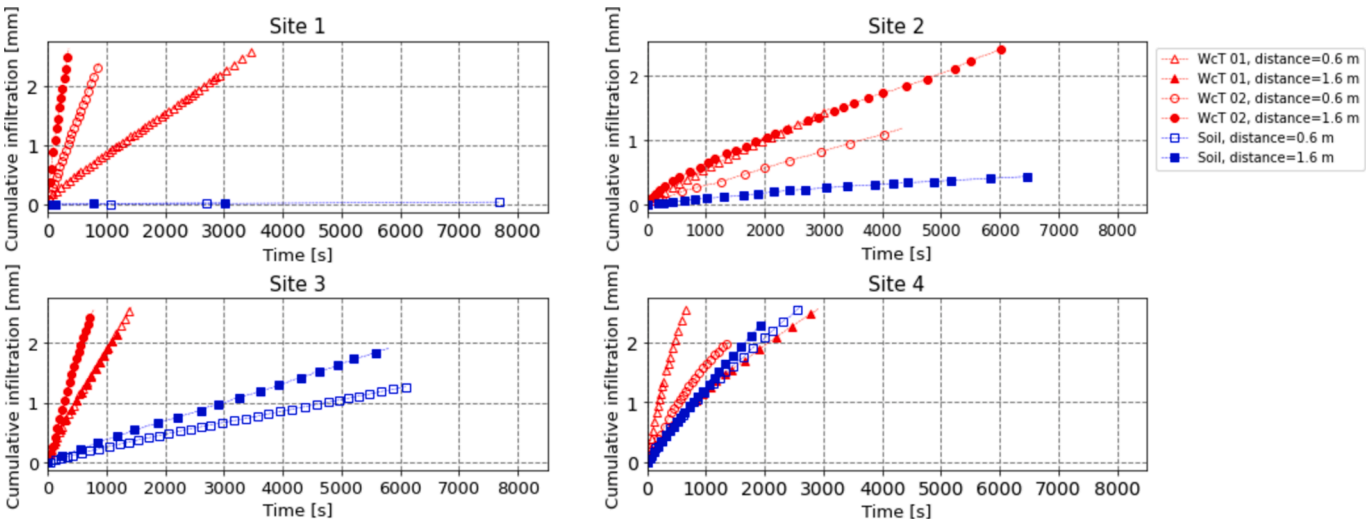

Fig. 3. Cumulative infiltration curves in the reference soils (blue) and woodchip-filled trenches (WcT) (red) for the four study sites. (For interpretation of the references to colour in this figure legend, the reader is referred to the web version of this article.)

Table 3
Average saturated hydraulic conductivity (Ks), as calculated using the BEST methods.

	Site 1						**Site 2**					
	Soil	Soil	WcT_1 (0.6 m)	WcT_1 (1.6 m)	WcT_2 (0.6 m)	WcT_2 (1.6 m)	Soil	Soil	WcT_1 (0.6 m)	WcT_1 (1.6 m)	WcT_2 (0.6 m)	WcT_2 (1.6 m)
Ks (m/s)	6.1E-07	8.3E-07	4.8E-05	Data not usable	1.4E-04	1.1E-04	2.9E-06	Data not usable	2.2E-05	Data not usable	1.9E-05	7.0E-06
IR (%)	–	–	6511	–	19,216	15,292	–	–	676	–	564	147
	Site 3						**Site 4**					
	Soil	Soil	WcT_1 (0.6 m)	WcT_1 (1.6 m)	WcT_2 (1.6 m)	WcT_2 (1.6 m)	Soil	Soil	WcT_1 (0.6 m)	WcT_1 (1.6 m)	WcT_2 (0.6 m)	WcT_2 (1.6 m)
Ks (m/s)	1.5E-05	1.9E-05	6.4E-05	4.9E-05	8.2E-05	Data not usable	6.8E-05	2.0E-05	3.6E-05	9.1E-06	1.0E-05	Data not usable
IR (%)	–	–	274	190	383	–	–	–	82	−54	−85	–

the infiltration ring was positioned at a depth of 0 cm, in the middle of the image.

For Site 1, the tracer is mainly located within the top 5 cm of the soil, with a few isolated stains below. The top layer stained with the dye would be expected to result from water flow through the matrix, corresponding to "matrix infiltration", whereby a wetting front forms and moves downward. In contrast, we would attribute the isolated stains below to isolated preferential flow through macropores (Cey et al., 2009, 2009). Site 2 displays a rather similar pattern to that of Site 1, with a sizable presence of tracer within the first 5 cm of soil and more diffuse stains below. The preferential flows seem even more isolated than those in Site 1. Sites 3 and 4 present a more heterogenous distribution across different depths. We could attribute these patterns either to matrix flow that extends deeper yet with some flow regionalization due to a specific soil organization (e.g. presence of various types of materials) or else to macropore flow with a denser macropore network. At Site 4, a few isolated stained regions appear below a depth of 10–15 cm.

3.3. Total soil porosity

Fig. 5 exhibits the porosity of both the reference soil and the soil below the WcT for the 4 study sites. In 3 out of 4 WcT samples, porosity is higher below the WcT than in the reference soil samples. For Site 1, the porosity equals approx. 0.29 $m^3\ m^{-3}$ for the reference soil, increasing by 38 % for the WcT. For Site 2, the porosity is approx. 0.39 $m^3\ m^{-3}$ for the reference soil, increasing between 10 % and 28 % for the WcT. For Site 3, the porosity is about 0.36 $m^3\ m^{-3}$ for the reference soil, increasing by 31 % to 69 % for the WcT. Lastly, the porosity at Site 4 is about 0.35 $m^3\ m^{-3}$ for the reference soil, with an increase of between 41 % and 100 % in the WcT.

As for Ks, no significant difference or systematic trend was observed between the samples close to the feeding point and those far from it. Conversely, we can note a clear increase in soil porosity between the reference soils and the soils below the WcT.

3.4. Soil chemical features

Fig. 6 displays the total organic carbon, total nitrogen and total phosphorous contents in the reference soils and the soils below the WcT at various depths from level 0 (0–5 cm, 5–10 cm and 10–20 cm). For reference soils from Sites 1 and 2, the TOC concentrations are fairly low and do not vary with depth. Given the thickness of the studied soil, the same horizon is being analyzed at each depth. For the reference soil from Site 3, the TOC concentration decreases with depth, thus indicating a change of horizon between 5 and 10 cm. This observation is consistent with the photographs taken during the dye tracer experiment, wherein the change in horizon is visible. For Site 4, the reference soil TOC decreases slightly with depth. These same trends were found for all reference soil parameters, apart from total phosphorus content at Site 2.

The presence of a woodchip-filled trench clearly impacts the profiles for all variables (TOC, TN, TP), mostly for sites 2 and 4. The values of all variables are increased below the WcT, in comparison with the reference soil, simultaneously coupled with an increase in the vertical gradient. TOC contents exhibit an increase of between + 7 % and + 1400 % over

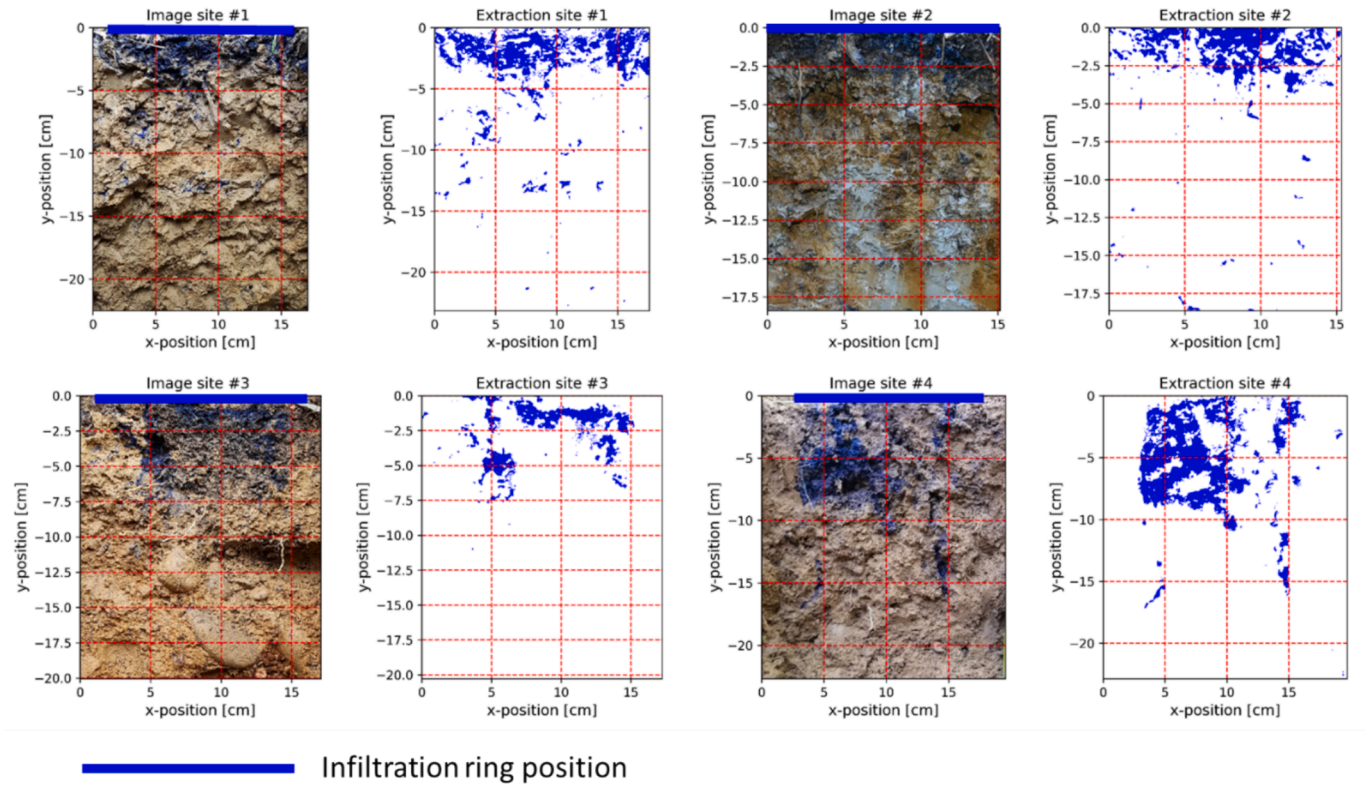

Fig. 4. Dye tracer and sand pit image analysis: Each site photograph shows the soil pit (left) and isolation of the stained regions (right). Only one photograph was obtained per site.

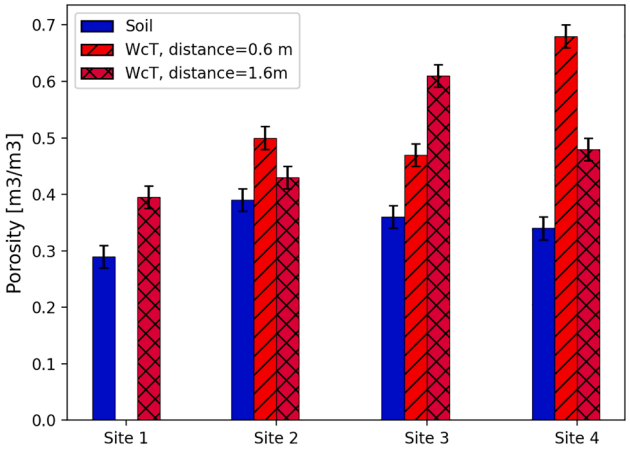

Fig. 5. Porosity in the reference soil (blue) and woodchip-filled trenches at both 0.6 m (light red) and 1.6 m (dark red) from the feeding point. (For interpretation of the references to colour in this figure legend, the reader is referred to the web version of this article.)

the first 5 cm. This effect is much more pronounced for the older sites (2 and 4) than the younger sites (1 and 3), with very tiny effects. This finding highlights the importance of time on the processes of organic matter transfer to the deeper layers. Time is needed to convey significant amounts of TOC due to woodchip degradation or gray water injection. As for TN content, a similar distinction can be drawn between Sites 2 and 4, on the one hand, and Sites 1 and 3, on the other. For the former (Sites 2 and 4), TN contents below the WcT are clearly higher than in the reference soils (from + 70 % to + 194 %), especially over the first 10 cm. For Sites 1 and 3, this increase is smaller or even near zero (from + 6 % to + 80 %). This link between age and changes in total nitrogen content beneath the trench could be indicative of slow processes that may take several years to set in. Another key parameter for soil characterization is the C/N ratio. To put our data into perspective, we could use a few reference values: for forest-type soils, C/N values below 25 indicate that the concentration of inorganic nitrogen compounds easily assimilated by trees (mainly nitrates) would be high enough to allow for their nutrition (Baize, 2018). For agricultural soils, demand is greater and the mineralization of nitrogen compounds is considered to encounter difficulties at C/N ratios > 12 (Baize, 2018). The reference soils have different C/N ratios: between 9.2 and 9.9 for Site 1, between 2.1 and 2.6 for Site 2, between 10 and 12 for Site 3, and about 9 for Site 4. On the whole, the C/N ratio increases for WcT compared to reference soils: between 6.8 and 17 for Site 1, between 2.2 and 13.4 for Site 2, between 9.37 and 12.9 for Site 3, and between 9.7 and 13.8 for Site 4. Regarding the total phosphorus contents below the WcT, the first 5 cm show a relatively low accumulation of phosphorus (between 0.1 and 0.3 g P/kg) for all sites except Site 4, where a maximum increase of 0.5 g/kg has been reached. Once again, this response could be correlated with the age of the filter and woodchip degradation.

Two groups would therefore seem to emerge, discriminated by age and TOC, TN, TP contents, namely: i) Sites 1 and 3, i.e., the younger sites, where TOC, NT and PT concentrations are quite similar between the reference soil and the soil below the WcT; and ii) Sites 2 and 4, the older sites, where the WcT contents are much higher than in the reference soils, especially within the top 10 cm, which demonstrates the impact of woodchips or gray water on soil quality.

3.5. *Earthworm abundance*

The last step in our methodology was the evaluation of macrofauna abundance. Table 4 displays the number of earthworms (all species) in both the reference soils and the soils under WcT. For Sites 1, 2 and 4, the number of earthworms is greater in the soils below WcT than in the reference soils (+66 % to + 700 %). Even though a species identification

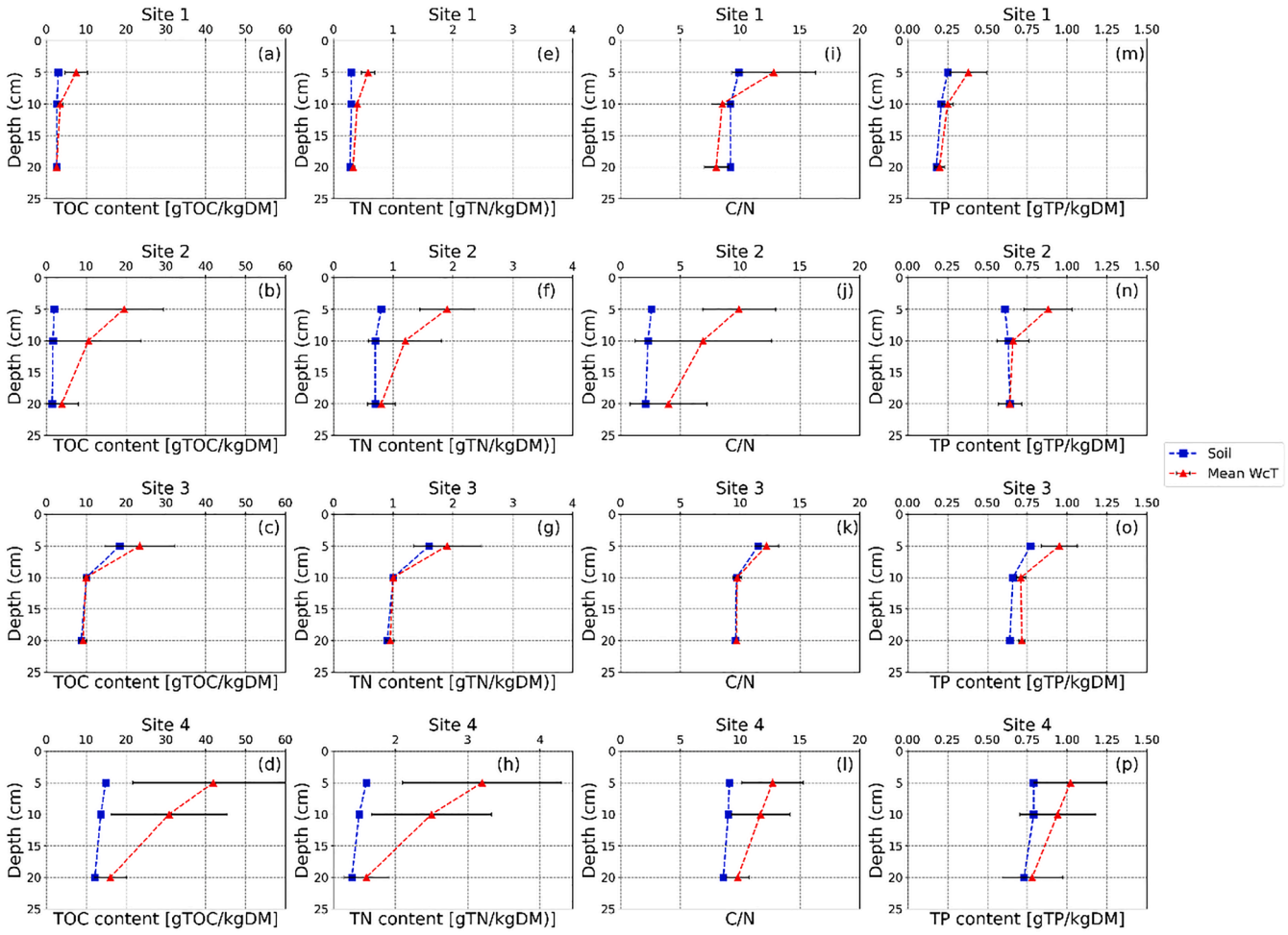

Fig. 6. (a-d) Total organic carbon (TOC), (e-h) total nitrogen (TN), (i-l) C/N ratio, and (m-p) total phosphorus (TP) contents both in the reference soils (blue) and below the woodchip-filled trenches (red). (For interpretation of the references to colour in this figure legend, the reader is referred to the web version of this article.)

Table 4
Counting of earthworms (number of individuals), cumulative number including all species, by a combined mechanical-chemical method in both the reference soils and the soils under woodchip-filled trenches (WcT).

	Site 1	Site 2	Site 3	Site 4
WcT	62	64	8	40
Reference soil	27	14	14	5

of the earthworms was not performed, it could be visually noted that the earthworms present in the WcT of Site 3 were larger and taller than those in the reference soil.

4. Discussion

4.1. Effects of woodchips on hydraulic conductivity

The results presented in the previous section showed that at Sites 1 and 2, under the WcT, a major increase affected the hydraulic conductivity at saturation. Ks increased by at least 150 % and, in some cases, up to 19000 %. For Site 3, the variations also reflected an increase in hydraulic conductivity at saturation, but to a lesser extent, with values increasing by values ranging from 150 % to 300 %. Lastly, for Site 4, the results do not show any clear and significant behavior. It should be noted that Site 4 is the oldest, as characterized by significantly longer feeding and resting periods (i.e., the time between two consecutive operation periods) compared to the other sites.

Briefly, our findings reveal that the woodchip-filled trenches tend to improve or, at least, maintain the hydraulic conductivity at saturation of the soil below the WcT. In all cases, it is considered that the hydraulic conductivity of the trench itself is quasi-infinite, in comparison to the soil below, hence the bulk hydraulic resistance of the whole stems from the hydraulic conductivity of the soil below as suggested by Lassabatere et al. (2010) and Slimene et al. (2017). For Sites 3 and 4, which show the least variations, it should be noted that their soils are quite similar with fairly equivalent compositions compared to Sites 1 and 2 (Table 2), which might suggest a link between performance and soil type. The soils at Sites 3 and 4 may present a texture and structure more propitious for water infiltration than the soils at Sites 1 and 2, since they are composed of coarser matrices with higher Ks, as depicted in Table 3. Note also that Site 4 is the oldest one studied and after ten years of operations, no major reduction in hydraulic conductivity seems to occur. These changes observed on the Ks are confirmed by the trends in porosities. Even though an increase in porosity does not always translate to an increase in hydraulic conductivity at saturation, the porosities clearly show an increasing trend across all sites, with values that can rise to the order of 0.5 to 0.6 $m^3.m^{-3}$. These results indicate that the parameters controlling the flow have evolved under the infiltration trenches in such a way that infiltration has been enhanced for all cases, with clearer effects for the native soils with lower saturated hydraulic conductivity.

4.2. How to explain the improvement in infiltration capacity?

The trend shown by the results indicates an improvement in

infiltration capacity. The dye tracer experiments from the Brilliant Blue clearly reveal preferential paths in the soil under the infiltration trenches. In the field, these deep stains appeared to be related to either earthworm galleries or macropores induced by roots. Presumably, the presence of water in the trenches and the woodchips haved enhance the development of plant roots. It also appears certain that the formed ecosystem favors the development of macrofauna, particularly earthworms. This finding has been confirmed by the larger number of earthworms in the woodchip trenches. Species identification may constitute a perspective for identifying the type of earthworms and predicting their effect on the soil structure It can also be noted that the enrichment in carbon and nitrogen of the soil, most likely due to both woodchip degradation and the contribution of domestic water and leachates, may have been enhanced by bioturbation. The bioturbation effect has already been demonstrated in other studies on other materials, e.g. biochar (Sadeghi et al., 2021). This enrichment in carbon can also favorably influence soil structure, in impacting its organization as well as hydraulic conductivity. In fact, the presence of organic matter in soil enables the formation of aggregates that stabilize soil structure, while increasing porosity and water retention capacity (Krull et al., 2004). Moreover, a higher concentration of organic carbon in the soil is generally associated with a higher concentration of microbial biomass and greater biodiversity on a global scale (FAO, 2020). A positive correlation often exists between the soil organic carbon content and biodiversity (FAO, 2020).

4.3. A woodchip infiltration trench beyond decentralized treatment

All results were obtained on decentralized sewage systems, providing quite obviously key perspectives on applications in France, a country with over 5 million decentralized installations (https://www.assainissement-non-collectif.developpement-durable.gouv.fr). In the context of climate change, the use of woodchips, a renewable material, for water infiltration has become a promising strategy. The initial results seem to show a strong potential for maintaining the infiltration capacity, which is also one of the main concerns in such a system. However, this article has limited the approach to specific soil types and therefore, at this stage, cannot be generalized to all soils. Further studies will be necessary for other soil types. It would also be worthwhile to compare this evolution with a gravel-filled trench. Unfortunately, we did not have at our disposal a site equally as old. Yet it should be noted that over a period of ten years of operations, the hydraulic performance of woodchip-filled trenches had been maintained; however, no information was available over a longer period, one with even greater woodchip degradation. Lastly, it is clear that the issue of maintaining infiltration capacity is indeed significant, although future work on the quality of the infiltrated water will be necessary; soil and groundwater quality are in fact at stake. These encouraging results also lead to valuable perspectives in other fields of application, e.g., the infiltration of rainwater and secondary treated effluents, or to manage aquifer recharge. For these applications, the use of woodchips could enrich the soil with carbon and limit the use of non-renewable materials in infiltration surfaces. However, due to the differences in frequency of water inflow and the nature of the water, the same conclusions might not be drawn, thus promoting an examination of the evolution in hydraulic properties of the soil with WcT for such new applications.

5. Conclusion

In order to respond to the challenge of maintaining UW infiltration capacity over time, this study has sought to demonstrate the potential benefits of woodchips as a drainage material in infiltration surfaces. The methodology applied to case studies has revealed an increase or preservation of the hydraulic conductivity at saturation for three types of soil under the infiltration trenches in decentralized systems. Through the results of dye tracer experiments and a characterization of earthworm abundance, the study has also highlighted the existence of preferential pathways, induced by earthworms present in large quantities in the WcT or root systems developed by plants. Chemical analyses of the soils showed a significant enrichment of carbon and nitrogen under the trench, which may also improve both soil structure and, indirectly, water infiltration capacity. All these analyses are suitable for the soil types studied as well as for systems in use for 5 to 10 years, yet further studies are needed to investigate other types of soil and effluent. These findings underscore the potential of woodchips in sustainable urban water management as a means of enhancing the functionality and efficiency of drainage materials through limiting the clogging effect and opening a wide range of perspectives for UW infiltration. However, this type of system, which was intended to be more sustainable, requires additional environmental analyses in order to both control nitrous oxide production and assess the impacts on the growth of surrounding plants.

CRediT authorship contribution statement

P. Louis: Writing – original draft, Visualization, Validation, Data curation, Conceptualization. **L. Delgado-Gonzalez:** Investigation, Data curation, Conceptualization. **L. Lassabatère:** Writing – review & editing, Validation, Supervision. **S. Czarnes:** Writing – review & editing, Validation. **J. Aubert:** Methodology, Conceptualization. **A. Imig:** Validation, Data curation. **R. Clément:** Writing – review & editing, Funding acquisition, Conceptualization.

Declaration of competing interest

The authors declare that they have no known competing financial interests or personal relationships that could have appeared to influence the work reported in this paper.

Data availability

Data will be made available on request.

Acknowledgments

This research study was funded by the French Ministry of Ecological Transition (MATCARB project). The project has also partially been supported by EUR H2O'Lyon (ANR-17-EURE-0018) at the Université de Lyon. Funding from the Research Federation BioEEnViS (FR3728) of Lyon/Saint-Etienne is also kindly acknowledged. The authors would like to thank the association Ecocentre Pierre et Terre, and in particular Christophe Merotto, for their tremendous assistance.

References

Angulo-Jaramillo, R., Bagarello, V., Di Prima, S., Gosset, A., Iovino, M., Lassabatere, L., 2019. Beerkan Estimation of Soil Transfer parameters (BEST) across soils and scales. J. Hydrol. 576, 239–261. https://doi.org/10.1016/j.jhydrol.2019.06.007.

Assouline, S., Narkis, K., 2011. Effects of long-term irrigation with treated wastewater on the hydraulic properties of a clayey soil. Water Resour. Res. 47, 2011WR010498. https://doi.org/10.1029/2011WR010498.

Bagarello, V., Di Prima, S., Iovino, M., 2014. Comparing alternative algorithms to analyze the beerkan infiltration experiment. Soil Sci. Soc. Am. J. 78, 724–736. https://doi.org/10.2136/sssaj2013.06.0231.

Baize, D., 2018. Guide des analyses en pédologie. Éditions Quae.

Bisone, S., Gautier, M., Masson, M., Forquet, N., 2017. Influence of loading rate and modes on infiltration of treated wastewater in soil-based constructed wetland. Environ. Technol. 38, 163–174. https://doi.org/10.1080/09593330.2016.1185165.

Blouin, M., Hodson, M.E., Delgado, E.A., Baker, G., Brussaard, L., Butt, K.R., Dai, J., Dendooven, L., Peres, G., Tondoh, J.E., Cluzeau, D., Brun, J.-J., 2013. A review of earthworm impact on soil function and ecosystem services. Eur. J. Soil Sci. 64, 161–182. https://doi.org/10.1111/ejss.12025.

Boano, F., Caruso, A., Costamagna, E., Ridolfi, L., Fiore, S., Demichelis, F., Galvão, A., Pisoeiro, J., Rizzo, A., Masi, F., 2020. A review of nature-based solutions for greywater treatment: Applications, hydraulic design, and environmental benefits. Sci. Total Environ. 711, 134731. https://doi.org/10.1016/j.scitotenv.2019.134731.

Braud, I., De Condappa, D., Soria, J.M., Haverkamp, R., Angulo-Jaramillo, R., Galle, S., Vauclin, M., 2005. Use of scaled forms of the infiltration equation for the estimation

of unsaturated soil hydraulic properties (the Beerkan method). Eur. J. Soil Sci. 56, 361–374. https://doi.org/10.1111/j.1365-2389.2004.00660.x.
Brooks, R., Corey, A., 1964. Hydraulic Properties of Porous Media. Hydrol. Pap. Colo. State Univ.
Brun, F., Dubois, V., Boutin, C., 2021. L'emploi du broyat de bois, une solution durable pour traiterles eaux ménagères ?: Use of woodchips: a sustainable solution for the treatment of grey water? Tech. Sci. Méthodes 37–53. 10.36904/tsm/202103037.
Bünemann, E.K., Bongiorno, G., Bai, Z., Creamer, R.E., De Deyn, G., De Goede, R., Fleskens, L., Geissen, V., Kuyper, T.W., Mäder, P., Pulleman, M., Sukkel, W., Van Groenigen, J.W., Brussaard, L., 2018. Soil quality – A critical review. Soil Biol. Biochem. 120, 105–125. https://doi.org/10.1016/j.soilbio.2018.01.030.
Carsel, R.F., Parrish, R.S., 1988. Developing joint probability distributions of soil water retention characteristics. Water Resour. Res. 24, 755–769. https://doi.org/10.1029/WR024i005p00755.
Cey, E.E., Rudolph, D.L., Passmore, J., 2009. Influence of macroporosity on preferential solute and colloid transport in unsaturated field soils. J. Contam. Hydrol. 107, 45–57.
Chahar, B.R., Graillot, D., Gaur, S., 2012. Storm-water management through infiltration trenches. J. Irrig. Drain. Eng. 138, 274–281. https://doi.org/10.1061/(ASCE)IR.1943-4774.0000408.
Concialdi, P., Di Prima, S., Bhanderi, H.M., Stewart, R.D., Abou Najm, M.R., Lal Gaur, M., Angulo-Jaramillo, R., Lassabatere, L., 2020. An open-source instrumentation package for intensive soil hydraulic characterization. J. Hydrol. 582, 124492. https://doi.org/10.1016/j.jhydrol.2019.124492.
D'Aniello, A., Cimorelli, L., Cozzolino, L., Pianese, D., 2019. The effect of geological heterogeneity and groundwater table depth on the hydraulic performance of stormwater infiltration facilities. Water Resour. Manag. 33, 1147–1166. https://doi.org/10.1007/s11269-018-2172-5.
Delgado-Gonzalez, L., Forquet, N., Choubert, J.-M., Boutin, C., Moreau, M., Moreau, S., Clement, R., 2023. Flow path monitoring by discontinuous time-lapse ERT: An application to survey relationships between secondary effluent infiltration and roots distribution. J. Environ. Manage. 326. https://doi.org/10.1016/j.jenvman.2022.116839.
Di Prima, S., Lassabatere, L., Bagarello, V., Iovino, M., Angulo-Jaramillo, R., 2016. Testing a new automated single ring infiltrometer for Beerkan infiltration experiments. Geoderma 262, 20–34. https://doi.org/10.1016/j.geoderma.2015.08.006.
FAO, I., 2020. State of knowledge of soil biodiversity – Status, challenges and potentialities. Summary for policy makers.
Flury, M., Flühler, H., 1994. Brilliant Blue FCF as a dye tracer for solute transport studies—A toxicological overview. J. Environ. Qual. 23, 1108–1112. https://doi.org/10.2134/jeq1994.00472425002300050037x.
Fontana, M., Johannes, A., Zaccone, C., Weisskopf, P., Guillaume, T., Bragazza, L., Elfouki, S., Charles, R., Sinaj, S., 2023. Improving crop nutrition, soil carbon storage and soil physical fertility using ramial wood chips. Environ. Technol. Innov. 31, 103143. https://doi.org/10.1016/j.eti.2023.103143.
Haverkamp, R., Ross, P.J., Smettem, K.R.J., Parlange, J.Y., 1994. Three-dimensional analysis of infiltration from the disc infiltrometer. 2. Physically based infiltration equation. Water Resour. Res. 30, 2931–2935.
Hillel, D., 1980. Fundamentals of soil physics. Academic Press, New York.
Krull, E.S., Skjemstad, J.O., Baldock, J.A., 2004. Functions of Soil Organic Matter and the Effect on Soil Properties. Coop. Res. Cent. Greenh. Account, Canberra.
Lassabatere, L., Angulo-Jaramillo, R., Soria Ugalde, J.M., Cuenca, R., Braud, I., Haverkamp, R., 2006. Beerkan estimation of soil transfer parameters through infiltration experiments-BEST. Soil Sci. Soc. Am. J. 70, 521–532. https://doi.org/10.2136/sssaj2005.0026.
Lassabatere, L., Angulo-Jaramillo, R., Goutaland, D., Letellier, L., Gaudet, J.P., Winiarski, T., Delolme, C., 2010. Effect of the settlement of sediments on water infiltration in two urban infiltration basins. Geoderma 156, 316–325. https://doi.org/10.1016/j.geoderma.2010.02.031.
Lassabatere, L., Di Prima, S., Angulo-Jaramillo, R., Keesstra, S., Salesa, D., 2019. Beerkan multi-runs for characterizing water infiltration and spatial variability of soil hydraulic properties across scales. Hydrol. Sci. J. 64, 165–178. https://doi.org/10.1080/02626667.2018.1560448.
Maboeta, M.S., van Rensburg, L., 2003. Vermicomposting of industrially produced woodchips and sewage sludge utilizing Eisenia fetida. Ecotoxicol. Environ. Saf. 56, 265–270. https://doi.org/10.1016/S0147-6513(02)00101-X.
Nemes, A., Rawls, W.J., Pachepsky, Y.A., 2005. Influence of Organic Matter on the Estimation of Saturated Hydraulic Conductivity. Soil Science Society of America Journal 69, 1330–1337. https://doi.org/10.2136/sssaj2004.0055.
Rabouli, S., Serre, M., Dubois, V., Gance, J., Henine, H., Molle, P., Truffert, C., Delgado-Gonzalez, L., Clément, R., 2021. Spatialization of saturated hydraulic conductivity using the Bayesian Maximum Entropy method: Application to wastewater infiltration areas. Water Res. 204, 117607. https://doi.org/10.1016/j.watres.2021.117607.
Rawls, W.J., Nemes, A., Pachepsky, Ya., 2004. Effect of soil organic carbon on soil hydraulic properties, in: Developments in Soil Science, Development of Pedotransfer Functions in Soil Hydrology. Elsevier, pp. 95–114. https://doi.org/10.1016/S0166-2481(04)30006-1.
Sadeghi, S.H., Hazbavi, Z., Kiani-Harchegani, M., Younesi, H., Sadeghi, P., Angulo-Jaramillo, R., Lassabatere, L., 2021. The hydrologic behavior of Loess and Marl soils in response to biochar and polyacrylamide mulching under laboratorial rainfall simulation conditions. J. Hydrol. 592, 125620. https://doi.org/10.1016/j.jhydrol.2020.125620.
Schneider, A., Hirsch, F., Raab, A., Raab, T., 2018. Dye tracer visualization of infiltration patterns in soils on relict charcoal hearths. Front. Environ. Sci. 6, 143. https://doi.org/10.3389/fenvs.2018.00143.
Sharma, R., Malaviya, P., 2021. Management of stormwater pollution using green infrastructure: The role of rain gardens. WIREs Water 8, e1507. https://doi.org/10.1002/wat2.1507.
Slimene, E.B., Lassabatere, L., Šimůnek, J., Winiarski, T., Gourdon, R., 2017. The role of heterogeneous lithology in a glaciofluvial deposit on unsaturated preferential flow-a numerical study. J. Hydrol. Hydromech. 65, 209–221. https://doi.org/10.1515/johh-2017-0004.
Taylor, M.D., Kim, N.D., Hill, R.B., Chapman, R., 2010. A review of soil quality indicators and five key issues after 12 yr soil quality monitoring in the Waikato region. Soil Use Manag. 26, 212–224. https://doi.org/10.1111/j.1475-2743.2010.00276.x.
van Genuchten, M.T., 1980. A closed-form equation for predicting the hydraulic conductivity of unsaturated soils. Soil Sci. Soc. Am. J. 44, 892–898. https://doi.org/10.2136/sssaj1980.03615995004400050002x.
Yilmaz, D., Lassabatere, L., Angulo-Jaramillo, R., Deneele, D., Legret, M., 2010. Hydrodynamic characterization of basic oxygen furnace slag through an adapted BEST method. Vadose Zone J. 9, 107–116. https://doi.org/10.2136/vzj2009.0039.